INSTITUTE OF PHYSICS PUBLISHING JOURNAL OF NEURAL ENGINEERING
J. Neural Eng. **1** (2004) 63–71 PII: S1741-2560(04)76526-X

A brain–computer interface using electrocorticographic signals in humans*

Eric C Leuthardt[1,5], Gerwin Schalk[2], Jonathan R Wolpaw[2,3], Jeffrey G Ojemann[4] and Daniel W Moran[5]

[1] Department of Neurological Surgery, Barnes-Jewish Hospital, St Louis, MO 63110, USA
[2] Wadsworth Center, New York State Department of Health, Albany, NY 12201, USA
[3] State University of New York, Albany, NY 12222, USA
[4] Department of Neurological Surgery, University of Washington School of Medicine, Children's Hospital and Regional Medical Center, Seattle, WA 98105, USA
[5] Department of Biomedical Engineering, Washington University in St Louis, St Louis, MO 63130, USA

Received 24 February 2004
Accepted for publication 7 May 2004
Published 14 June 2004
Online at stacks.iop.org/JNE/1/63
doi:10.1088/1741-2560/1/2/001

Abstract
Brain–computer interfaces (BCIs) enable users to control devices with electroencephalographic (EEG) activity from the scalp or with single-neuron activity from within the brain. Both methods have disadvantages: EEG has limited resolution and requires extensive training, while single-neuron recording entails significant clinical risks and has limited stability. We demonstrate here for the first time that electrocorticographic (ECoG) activity recorded from the surface of the brain can enable users to control a one-dimensional computer cursor rapidly and accurately. We first identified ECoG signals that were associated with different types of motor and speech imagery. Over brief training periods of 3–24 min, four patients then used these signals to master closed-loop control and to achieve success rates of 74–100% in a one-dimensional binary task. In additional open-loop experiments, we found that ECoG signals at frequencies up to 180 Hz encoded substantial information about the direction of two-dimensional joystick movements. Our results suggest that an ECoG-based BCI could provide for people with severe motor disabilities a non-muscular communication and control option that is more powerful than EEG-based BCIs and is potentially more stable and less traumatic than BCIs that use electrodes penetrating the brain.

M This article features online multimedia enhancements

1. Introduction

Brain–computer interfaces (BCIs) convert brain signals into outputs that communicate a user's intent [1]. Because this new communication channel does not depend on peripheral nerves and muscles, it can be used by people with severe motor disabilities. BCIs can allow patients who are totally paralyzed (or 'locked in') by amyotrophic lateral sclerosis (ALS), brainstem stroke or other neuromuscular diseases to express their wishes to the outside world. However, practical applications of BCI technology to the needs of people with severe disabilities are impeded by the limitations and requirements of current BCI methodologies.

BCIs can use non-invasive or invasive methods. Non-invasive BCIs use electroencephalographic activity (EEG) [2–7] recorded from the scalp. They are convenient, safe and inexpensive, but they have relatively low spatial resolution [8, 9], are susceptible to artifacts such as electromyographic (EMG) signals, and often require extensive user training. Invasive BCIs use single-neuron activity recorded within the brain [10–13]. While they have higher spatial resolution and might provide control signals with many degrees of freedom, BCIs that depend on electrodes within cortex face substantial problems in achieving and maintaining stable

* The authors declare that they have no competing financial interests.

Table 1. Clinical profiles. All patients were literate and functionally independent. During the period in which ECoG data were collected, patient A was acutely impaired (e.g., in speech fluency, attention and response times) by slow post-operative recovery. None of the patients had a traumatic or structural lesion that was responsible for their seizures (i.e., all had idiopathic epilepsy).

Patient	Age	Sex	Cognitive/motor capacity	Seizure type	Seizure focus
A	28	M	Moderately impaired	GTC	Frontal lobe
B	23	M	Normal range	CP	Left middle TL
C	35	F	Normal range	CP	Left inferior and mesial TL
D	33	M	Mildly impaired	CP & GTC	Left middle and posterior TL

Abbreviations: M, male; F, female; GTC, secondarily generalized tonic-clonic; CP, complex partial; TL, temporal lobe.

long-term recordings. The small, high-impedance recording sites make penetrating electrodes susceptible to signal degradation due to encapsulation [14]. Also, small displacements of the tiny penetrating electrodes can move the recording sites away from the cortical layers that contain the large easily recorded neurons, such as pyramidal neurons in layer 5 of motor cortex. These issues are crucial obstacles that currently prohibit their clinical use in humans.

An intermediate BCI methodology, using electrocorticographic activity (ECoG) recorded from the cortical surface, could be a powerful and practical alternative to these extremes. ECoG has higher spatial resolution than EEG (i.e., tenths of millimeters versus centimeters [8]), broader bandwidth (i.e., 0–200 Hz versus 0–40 Hz), higher amplitude (i.e., 50–100 μV maximum versus 10–20 μV), and far less vulnerability to artifacts such as EMG [8, 9, 15]. At the same time, because ECoG is recorded by subdural electrode arrays and thus does not require electrodes that penetrate into cortex, it is likely to have greater long-term stability and might also be safer than single-neuron recording [16, 17].

This study set out to explore the potential value for BCI applications of ECoG activity recorded over sensorimotor cortex in humans. We studied four patients in whom subdural electrode arrays were implanted for 3–8 days in preparation for surgery to remove an epileptic focus (see table 1 for clinical profiles). All four provided informed consent for the study, which had been reviewed and approved by the Washington University School of Medicine Institutional Review Board. The experimental approach was developed based on current understanding of sensorimotor rhythms and on the methodology of current EEG-based BCIs that use these rhythms [18] (see [1] for review). Sensorimotor rhythms comprise μ (8–12 Hz), β (18–26 Hz) and γ (>30 Hz) oscillations [6, 19–22]. They are thought to be produced by thalamocortical circuits and they change in amplitude in association with actual or imagined movements [22–26]. BCIs based on EEG oscillations have focused exclusively on μ and β rhythms because γ rhythms are inconspicuous at the scalp [27]. In contrast, γ rhythms as well as μ and β rhythms are prominent in ECoG [22–26]. This paper is the first report of a study that applies ECoG activity to online operation of a BCI system. We identified the locations and frequency bands of ECoG sensorimotor rhythms associated with specific movements or speech, or with imagery of those actions, and then determined whether people could learn to use these rhythms to control a cursor on a computer screen (see section 4 for additional details).

The principal results show that people can quickly learn to use the ECoG activity associated with imagery to control a cursor. Furthermore, additional data show that γ rhythms that are prominent in ECoG, but not in scalp EEG, are highly correlated with the direction of joystick movements in two dimensions. These results indicate that an ECoG-based BCI could provide control that is more precise and more quickly acquired than that provided by EEG-based BCIs, and at the same time may have signal stability advantages over BCIs that use microelectrodes implanted in cortex. Thus, BCI methods based on ECoG might prove to be of substantial value and thereby considerably extend and facilitate the application of BCI technology to the communication and control needs of people with severe motor disabilities.

2. Results

2.1. ECoG control of one-dimensional cursor movement

To select the sensorimotor rhythms to be used for online cursor control, we recorded ECoG from 32 electrodes over the left frontal-parietal-temporal cortex (see example in figure 1) while each patient performed each of six tasks: three motor actions (i.e., opening and closing right or left hand, protruding the tongue, saying the word 'move') and imagining each of these actions. For each electrode location, we derived by autoregressive spectral analysis [28] the voltage spectra from 0 to 200 Hz for each task and for the between-task inactive period. We compared each task to the inactive period and calculated the r^2 of the corresponding spectra (i.e., the proportion of the signal variance that was accounted for by the task) [29]. As expected [23], each task in each patient was typically associated with decreased μ and β rhythm amplitudes and increased γ rhythm amplitude at several locations over pre-frontal, pre-motor, sensorimotor and/or speech areas [30, 31]. The spatial and spectral foci of task-related ECoG activity, as revealed in the r^2 analysis, were usually similar for action and for imagination of the same action (e.g., saying the word 'move' and imagining saying the word 'move') [32].

For each patient, we selected one or two electrodes and up to four μ, β and/or γ frequency bands that showed the highest correlations with one of the three actions or imagery tasks described above (i.e., the ECoG features that had the

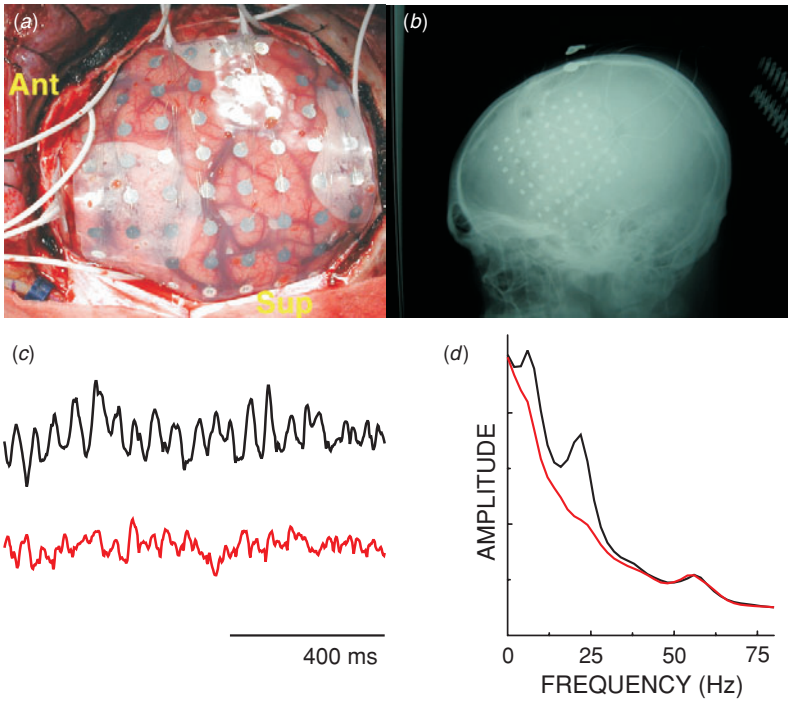

Figure 1. Examples of electrode placement and ECoG signals. (*a*) Intra-operative placement of a 64-electrode subdural array. Inter-electrode spacing was 1 cm and electrode diameter was 2 mm; Ant: anterior. (*b*) Post-operative lateral skull radiograph showing grid placement. (*c*) Raw ECoG signals from patient C during control of cursor movement. Black and red traces are from one of the electrodes that controlled cursor movement and are examples for the patient resting and imagining saying the word 'move', respectively. (*d*) Spectra for the corresponding conditions for the final run of online performance. Imagery is associated with decrease in μ (8–12 Hz) and β (18–26 Hz) frequency bands.

Table 2. Actions and imagined actions, electrode locations and ECoG frequency bands used for ECoG control of one-dimensional cursor movement, and final accuracies of that control. Brodman's areas were calculated using skull radiographs and a Talairach atlas [48].

Patient	Action or imagined action	Brodman's area	Frequency band (Hz)	Amplitude	Final accuracy
A	Opening and closing right hand	2	10.5–18.5	Decrease	74%
		2	48.5–54.5	Increase	
		3	30.5–34.5	Increase	
		3	48.5–50.5	Increase	
B	Imagining opening and closing right hand	3	30.5–32.5	Decrease	83%
C	Imagining saying 'move'	9, 44	20.5–22.5	Decrease	97%
D	Saying 'move'	6, 45	12.5–14.5	Decrease	93%
		6, 45	26.5–28.5	Decrease	
		6, 45	34.5–36.5	Decrease	
	Imagining saying 'move'	6, 45	12.5–14.5	Decrease	97%
		6, 45	26.5–28.5	Decrease	
		6, 45	34.5–36.5	Decrease	
	Protruding the tongue	45	12.5–14.5	Decrease	100%
	Imagining protruding the tongue	45	12.5–14.5	Decrease	84%

highest values of r^2). Patients then used the amplitudes of these features to control cursor movement in an online BCI protocol in which the objective was to move the cursor up or down to a target located in the upper or lower half of the screen. For example, patient B imagined right hand movement to move the cursor up, and rested to move it down (see online supplementary movie 1 at stacks.iop.org/JNE/1/63). The accuracy expected if patients lacked any ECoG control was 50%.

Patients completed one to eight 3 min runs separated by 1 min breaks. Each run comprised 33 individual trials (5.5 s per trial). Over these short training periods (3–24 min), all four patients achieved significant control of the cursor (74–100% final accuracy). Table 2 summarizes all results and figures 2 and 3 show analyses for the subset of results in which patients used imagined actions to control the system. We focus on imagined actions (rather than real actions) because they are most relevant to BCI use by people who are paralyzed.

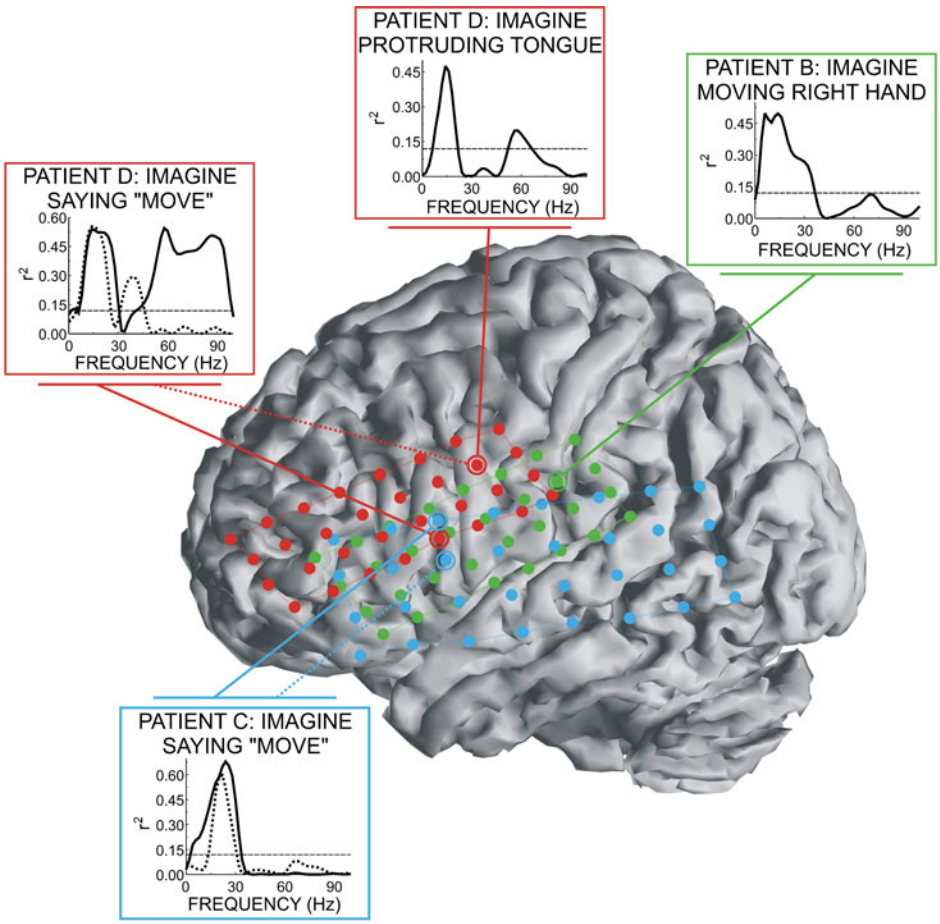

Figure 2. ECoG control of vertical cursor movement using imagination of specific motor or speech actions to move the cursor up and rest to move it down. The electrodes used for online control are circled and the spectral correlations of their ECoG activity with target location (i.e., top or bottom of screen) are shown. Grids for patients B, C and D are green, blue and red, respectively. The particular imagery tasks used are indicated. The substantial levels of control achieved with different types of imagery are evident. (The dashed lines indicate significance at the $p = 0.01$ level.) Correlations were calculated for the final two runs of online performance. Two different locations are shown for patients C and D: the solid and dotted r^2 spectra correspond to the sites indicated by the solid and dotted line locators, respectively. Grid locations were determined using stereotactic coordinates derived from a lateral skull radiograph and subsequently mapped to a standardized brain with a Talairach transformation (http://ric.uthscsa.edu/projects/talairachdaemon.html). The three-dimensional brain model was derived from MRI data [49].

Figure 2 illustrates for the final runs the strong correlation between the goal (i.e., moving the cursor up or moving it down) and the ECoG activity that controlled cursor movement. Figure 3 shows the rapid improvements in accuracy over the brief periods of study.

2.2. ECoG correlation with direction of two-dimensional joystick movement

In addition to the online BCI operation described above, ECoG was recorded while each patient used a joystick to move a cursor from the center of a computer screen to a target at one of 4 or 8 locations spaced around the periphery of the screen. For each electrode, we compared the 0–200 Hz ECoG spectra for joystick movement and for rest. All four patients showed at one or more electrodes significant spectral changes (i.e., $r^2 > 0.1$) between these conditions. We also compared the spectra for different directions of movement (e.g., right versus left). In patients B and D, we found μ, β and/or γ frequency bands at specific electrodes that were strongly correlated with movement direction. (Patient A had great difficulty executing the joystick task due to acute (i.e., post-operative) and chronic cognitive impairment. In patient C, the electrode grid was placed very low (see figure 2) so that it barely touched the lateral edge of the hand area.) Figures 4(*a*)–(*c*) illustrate with data from patient D the ECoG correlations with movement direction. It displays the correlations both immediately before movement (i.e., the movement preparation period) and during movement.

In further offline analyses of the joystick data from patients B and D, we used the ECoG features (i.e., amplitudes in specific frequency bands at specific electrodes) that had the highest correlations with movement direction as the input features to a neural network with no hidden layer and two linear output neurons. The network was trained to predict the vertical and horizontal directions of joystick movement. (One output neuron predicted horizontal direction and the other one vertical direction.) As shown in table 3 and figure 4(*d*),

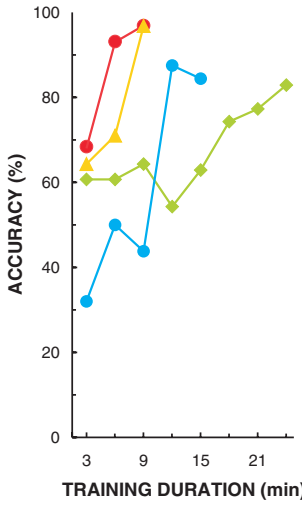

Figure 3. Learning curves for ECoG control of vertical cursor movement using motor imagery to move up and rest to move down (see text). (Accuracy in the absence of control would be 50%.) Patient B (—) imagined opening and closing the right hand, patients C (—) and D (—) imagined saying the word 'move', and patient D (—) imagined protruding the tongue. In each case, the rapid acquisition of control is evident and statistically significant by X^2 contingency test ($p < 0.05$, <0.005, <0.005 and <0.001, respectively). (Note: patient A, who was cognitively impaired by a slow post-operative recovery, only used actual movement in closed-loop control; thus, this figure does not include data for this patient.)

the predictions were highly correlated with the actual movement directions and generally showed substantial generalization to other data sets.

These joystick results, combined with the finding that both real and imagined motor actions show strong ECoG correlations, suggest that people could use ECoG activity recorded from a few properly selected sites for rapid and accurate multi-dimensional control of cursor movement.

3. Discussion

This study demonstrates for the first time rapid learning during closed-loop real-time control of cursor movements using ECoG activity associated with motor or speech imagery (figure 3). Using signal analysis and cursor control methods that were developed in BCI studies employing scalp-recorded EEG activity [33–36], this study found that ECoG-based control develops more quickly than EEG-based control [37, 38], and is likely to be substantially more effective in providing communication and control to people with severe motor disabilities.

Offline analysis of ECoG data recorded during a two-dimensional (2D) center-out joystick task showed substantial directional information (figure 4). Since Fetz and Finocchio's 1971 study showed that a motor cortical neuron can be used to control movement in a single dimension, researchers have strived to expand this to multiple dimensions [39]. In 1986, Georgopoulos and colleagues identified an accurate representation of three-dimensional arm movements in motor cortex, and proposed an effective decoding algorithm for predicting arm movements from a population of motor cortical neurons [11]. Due to technological limitations preventing real-time recording and analysis of data from many individual cortical neurons simultaneously, it was not until 2002 that Schwartz and colleagues became the first to obtain three-dimensional closed-loop, real-time control of a cursor in a monkey [13]. In 1994, Wolpaw and McFarland demonstrated significant two-dimensional control with scalp-recorded EEG signals in human subjects [37], and in current work they are achieving EEG-based two-dimensional control comparable to that reported in monkey single-neuron studies [38]. This EEG-based control relies on substantial training to establish two independent control signals (i.e., for vertical and horizontal movements, respectively) that are not evident prior to training. The two-dimensional joystick task used in the present study was similar to a wide variety of planar hand movements typically coordinated by the brain, and analysis revealed directionally specific ECoG activity at frequencies well above those usually discernible in scalp-recorded EEG. In combination with the finding that ECoG correlations with motor imagery and with actual movement are similar to each other, the joystick data suggest that ECoG activity comparable to that normally associated with behaviors such as joystick control could support more natural BCI operation that requires less training and achieves superior control.

The superiority of ECoG over EEG in reflecting movement direction results in large part from its greater

Table 3. Neural-network prediction of the direction of joystick movement from ECoG activity. Patients moved a cursor towards a target at one of 4 or 8 locations (i.e., center-out task). The amplitudes in 10 Hz bands at 3 or 4 electrode locations were the input features to a neural network (see text) that attempted to predict the vertical and horizontal directions of joystick movement. Columns A, B and C show the high correlations between actual horizontal and vertical movements and the neural-network predictions of these movements. (In the case of 8 targets, these calculations were done for the subset of 4 targets that were the same as the targets in the 4-target task.) In A, the network was trained on the whole data set and gave predictions for the same data set. In B, the network was trained on the first half of the data and gave predictions for the second half. In C, the network was trained on the even trials and gave predictions for the odd trials. The network predictions obtained from one data set generally show substantial generalization to another data set. (The last column shows the values of r^2 that are significant at the 0.01 level.)

				A		B		C		Significance level
Subject	No of trials	Frequencies (Hz)	No of locations	$r^2(x)$	$r^2(y)$	$r^2(x)$	$r^2(y)$	$r^2(x)$	$r^2(y)$	(r^2 for $p < 0.01$)
B (4 targets)	326	40–110	3	0.47	0.45	0.02	0.14	0.13	0.11	0.05
D (4 targets)	556	40–100	4	0.61	0.57	0.45	0.45	0.54	0.49	0.03
D (8 targets)	924	70–160	4	0.65	0.26	0.50	0.06	0.59	0.10	0.035

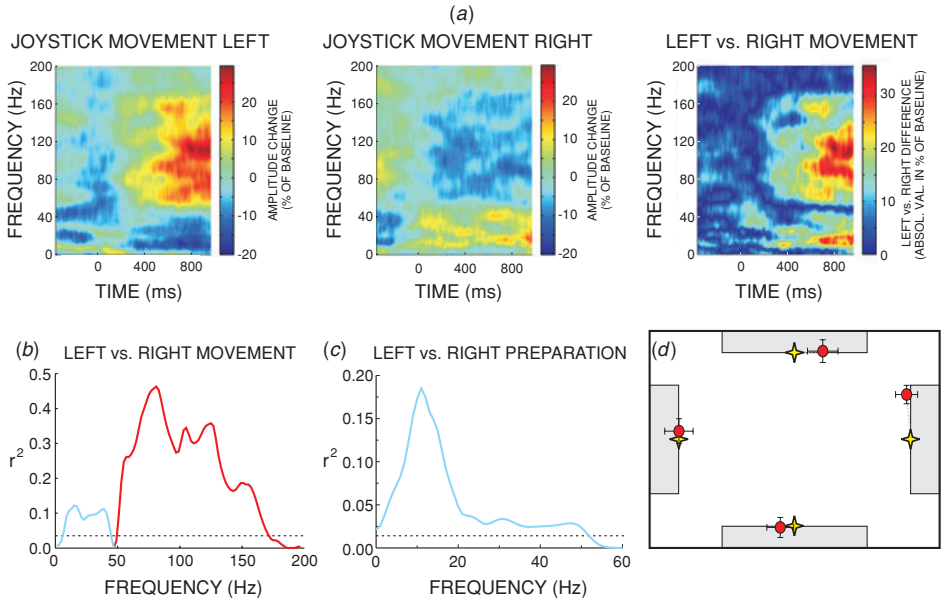

Figure 4. ECoG correlations with joystick movement direction before and during movement for patient D. At −400 ms the target appeared, and at 0 ms the cursor appeared and began to move controlled by the joystick. The patient's task was to move the cursor to a target at one of 4 or 8 locations (i.e., center-out task). (Figures (*a*)–(*c*) are based on the 8-location data set and are calculated for the left-most and right-most target; (*d*) is based on the 4-location data set.) (*a*) Left and center panels: time courses for left and right movements, respectively, of the amplitudes from 0–200 Hz of the difference between two adjacent electrodes. Right panel: the absolute value of the difference between left and right time courses. Movement direction is reflected in ECoG across a wide frequency range, including frequencies far above the EEG frequency range. In general, amplitudes at frequencies below and above 50 Hz change in opposite directions. (*b*) The correlation between the signal shown in (*a*) and movement direction over the period of movement execution. Correlation is much higher at higher frequencies not discernible in scalp EEG. (*c*) Correlation (for a single electrode location versus the remote reference electrode) with movement direction for the 400 ms prior to cursor movement. μ rhythm activity predicts movement direction. (In (*b*) and (*c*), ▬ and ▬ indicate negative correlation and positive correlation, respectively, with the amplitude of left movement minus right movement; and dashed lines indicate the value of r^2 that is significant at the 0.01 level.) (*d*) Average final cursor positions (●) predicted by a neural network from ECoG activity are close to the actual average final cursor positions (✦) (see text). (Error bars indicate the standard error of the mean.)

frequency range. As figure 4 illustrates, the ECoG frequencies that best reflected the movement direction were in the high γ range (i.e., 40–180 Hz), well above the frequency range (up to 40–50 Hz) readily discernible in the scalp-recorded EEG. ECoG's superior frequency range is attributable to two factors. First, the capacitance of cell membranes of the overlying tissue combined with their intrinsic electrical resistance constitutes a low-pass (RC) filter that largely eliminates higher frequencies from the EEG [27]. Second, higher frequencies tend to be produced by smaller cortical assemblies [40]. Thus, they are more prominent at electrodes that are closer to cortex than EEG electrodes and thereby achieve higher spatial resolution [8, 9].

ECoG directional representation is likely to be further improved by using a grid with closer electrode spacing. The 1 cm inter-electrode distance in the grids used here is significantly larger than the suggested optimum ECoG spatial sampling resolution of 1.25 mm [8]. Indeed, we often observed correlations limited to one or two recording sites. Thus, recording with higher spatial resolution might substantially improve ECoG-based BCI operation and facilitate control of multi-dimensional movements.

Although the origin and nature of ECoG/EEG electrical oscillations are not fully understood, our results are, in general, consistent with the conventional overlapping homunculus model of cortical functional anatomy. The frequency changes elicited with various actual and imagined motor actions are consistent with previous evidence that during sensorimotor function (including speech), μ and β rhythm amplitudes tend to decrease while γ rhythm amplitudes tend to increase [23, 41–44].

In summary, ECoG is likely to be an excellent BCI modality because it has higher spatial resolution, better signal-to-noise ratio, wider frequency range and lesser training requirements than scalp-recorded EEG, and at the same time may have greater long-term stability of signal quality over intracortical recording. By demonstrating the first use of ECoG for online operation of a BCI system and by showing its correlations with multi-dimensional movements, our results support these expectations. Further development of ECoG-based BCI methodology could greatly increase the power and practicality of BCI applications that can serve the communication and control needs of people with motor disabilities.

4. Methods

4.1. Subjects and experimental paradigms

The subjects in this study were four patients with intractable epilepsy who underwent temporary placement of intracranial

electrode arrays to localize seizure foci prior to surgical resection. They included three men (patients A, B and D) and one woman (patient C) (see table 1 for additional information.) All gave informed consent. The study was approved by the Human Studies Committee of Washington University Medical Center. Prior to this study, these patients had not been trained on a BCI system.

Each patient had a 48- or 64-electrode grid placed over the left frontal-parietal-temporal region including parts of sensorimotor cortex. These grids consisted of electrodes with a diameter of 2 mm and an inter-electrode distance of 1 cm (see figure 1). Grid placements and duration of ECoG monitoring were based solely on the requirements of the clinical evaluation, without any consideration of this study. Following placement of the subdural grid, each patient had post-operative anterior–posterior and lateral radiographs to verify its location.

4.2. Data collection

Each patient sat in a hospital bed about 75 cm from a video screen. In all experiments, we recorded ECoG from 32 electrodes (i.e., the upper part of the implanted grid) using the general-purpose BCI system BCI2000 [43]. All electrodes were referenced to an inactive electrode located over the temporal lobe far from the electrodes, amplified, bandpass filtered (0.1–220 Hz), digitized at 500 Hz, and stored. The amount of data obtained varied from patient to patient, and depended on the patient's physical state and willingness to continue.

Initial evaluations determined which ECoG features (i.e., amplitudes in particular frequency bands at particular electrode locations) were correlated with a particular movement, speech or motor imagery task. In each of eighteen 2 min runs, the patient was asked to perform one of six tasks (i.e., three runs for each task). The six tasks were as follows: open and close the right or left hand, protrude the tongue, say the word 'move' and imagine performing each of these three actions. In each run, the patient performed about 30 repetitions of the required task in response to a visual cue that lasted 2–3 s (during this interval, the patient repeated the task continuously), and rested when the screen was blank for 1 s. In two additional runs, patients were simply asked to rest with eyes open and closed, respectively.

We then conducted closed-loop BCI experiments in which the patient received online feedback that consisted of one-dimensional cursor movement controlled by ECoG features that had shown correlation with one of the six tasks. The ECoG features were integrated over time to yield the current cursor position (i.e., ECoG activity was treated as vertical velocity information [18]). Data were collected from each patient for one to eight 3 min runs, each comprised of 21–37 trials. The runs were separated by 1 min breaks. Each trial began with the appearance of a target that occupied either the top or bottom half of the right edge of the screen (randomly chosen throughout the run). One second later, the cursor appeared in the middle of the left edge of the screen and then moved steadily across the screen over a fixed period of 2.1–6.8 s with its vertical movement controlled continuously by the patient's ECoG features. The patient's goal was to move the cursor vertically so that it hit the appropriate (i.e., upper or lower) half of the screen when it reached the right edge. At 0.5 s after the cursor reached the right edge of the screen, the screen went blank, signaling the end of the trial. After a pause of 1 s, the next trial started. Accuracy expected in the absence of any control was 50%.

Finally, in three additional 3 min runs (about 50 trials each), the patient used a joystick (with the hand contralateral to the implanted electrode array) to move the cursor in two dimensions from the center of the screen to a target at one of four possible locations (i.e., a 'center-out' joystick task; figure 4(*d*)). One patient completed an additional 13 joystick runs with 8 target locations.

4.3. Identification of ECoG features to be used for online cursor control

From spectral analysis of the data gathered from each of the 32 electrodes with each of the six tasks, we identified the frequency bands in which amplitude was different between the task and rest. For these analyses, the time-series ECoG data were converted into the frequency domain using an autoregressive model of order 18. We calculated spectral amplitudes between 0 and 200 Hz in 2 Hz bins. Those electrodes and frequency bins with the most significant task-related amplitude changes (i.e., the highest values of r^2) were identified as features to be used to control cursor movement in the subsequent online BCI experiments.

The same analysis methods were applied to the data gathered during joystick movements in order to compare right versus left movement, up versus down movement, and movement versus rest.

4.4. ECoG control of vertical cursor movement online

The cursor moved vertically every 40 ms controlled by a translation algorithm based on a weighted, linear summation of the amplitudes in the identified frequency bands from the identified electrodes for the previous 280 ms (as developed for EEG-based control [18, 45, 46]). The weights were chosen so that this translation algorithm moved the cursor up with task execution (e.g., imagining tongue protrusion) and down with rest. This relationship was explained to the patient prior to these experiments.

4.5. Anatomical and functional mapping

Radiographs were used to identify the stereotactic coordinates of each grid electrode [47], and cortical areas were defined using Talairach's *Co-Planar Stereotaxic Atlas of the Human Brain* [48]. After the experiments described above, each patient underwent stimulation mapping to identify motor and speech cortices as part of his/her clinical care. In this mapping, 1 ms 5–10 mA square current pulses were passed through paired electrodes to induce sensation and/or evoke motor responses (including speech arrest). The experimental results described above were collated with these anatomical and functional mapping data. The topographical correlations

between electrical stimulation and movement or imagery were not strong enough to support clear conclusions (see online supplementary figure 1 at stacks.iop.org/JNE/1/63 for more information).

Acknowledgments

We thank Dr Ralph G Dacey for strong departmental support, Dr Jonathan S Carp, Dr Dennis J McFarland, Ms Theresa M Vaughan and Dr Elizabeth Winter Wolpaw for valuable advice throughout this work and for helpful comments on the manuscript, Dr Frank Gilliam for patient support, Ms Lucy Sullivan for ECoG technical support, and Dr Febo Cincotti for the three-dimensional brain model in figure 3. This work was supported in part by grants from NIH (NS41272 (JO), HD30146 (JRW) and EB00856 (JRW)), the McDonnell Center for Higher Brain Function (JO), and the James S McDonnell Foundation (ECL and JRW).

References

[1] Wolpaw J R, Birbaumer N, McFarland D J, Pfurtscheller G and Vaughan T M 2002 Brain–computer interfaces for communication and control *Clin. Neurophysiol.* **113** 767–91

[2] Vidal J J 1977 Real-time detection of brain events in EEG *IEEE Proc.* **65** 633–64 (special issue on biological signal processing and analysis)

[3] Sutter E E 1992 The brain response interface: communication through visually-induced electrical brain responses *J. Microcomput. Appl.* **15** 31–45

[4] Elbert T, Rockstroh B, Lutzenberger W and Birbaumer N 1980 Biofeedback of slow cortical potentials: I *Electroencephalogr. Clin. Neurophysiol.* **48** 293–301

[5] Farwell L A and Donchin E 1988 Talking off the top of your head: toward a mental prosthesis utilizing event-related brain potentials *Electroencephalogr. Clin. Neurophysiol.* **70** 510–23

[6] Wolpaw J R, McFarland D J, Neat G W and Forneris C A 1991 An EEG-based brain–computer interface for cursor control *Electroencephalogr. Clin. Neurophysiol.* **78** 252–9

[7] Pfurtscheller G, Flotzinger D and Kalcher J 1993 Brain–computer interface—a new communication device for handicapped persons *J. Microcomput. Appl.* **16** 293–9

[8] Freeman W J, Holmes M D, Burke B C and Vanhatalo S 2003 Spatial spectra of scalp EEG and EMG from awake humans *Clin. Neurophysiol.* **114** 1053–68

[9] Srinivasan R, Nunez P L and Silberstein R B 1998 Spatial filtering and neocortical dynamics: estimates of EEG coherence *IEEE Trans. Biomed. Eng.* **45** 814–26

[10] Kennedy P R and Bakay R A 1998 Restoration of neural output from a paralyzed patient by a direct brain connection *Neuroreport* **9** 1707–11

[11] Georgopoulos A P, Schwartz A B and Kettner R E 1986 Neuronal population coding of movement direction *Science* **233** 1416–9

[12] Laubach M and Wessberg J 2000 Cortical ensemble activity increasingly predicts behavior outcomes during learning of a motor task *Nature* **405** 567–71

[13] Taylor D M, Tillery S I and Schwartz A B 2002 Direct cortical control of 3D neuroprosthetic devices *Science* **296** 1829–32

[14] Shain W *et al* 2003 Controlling cellular reactive responses around neural prosthetic devices using peripheral and local intervention strategies *IEEE Trans. Neural Syst. Rehabil. Eng.* **11** 186–8

[15] Boulton A A, Baker G B and Vanderwolf C H (ed) 1990 *Neurophysiological Techniques: II. Applications to Neural Systems* (Totowam, NJ: Humana)

[16] Margalit E *et al* 2003 Visual and electrical evoked response recorded from subdural electrodes implanted above the visual cortex in normal dogs under two methods of anesthesia *J. Neurosci. Methods* **123** 129–37

[17] Pilcher W H and Rusyniak W G 1993 Complications of epilepsy surgery *Neurosurg. Clin. N. Am.* **4** 311–25

[18] Wolpaw J R, McFarland D J, Vaughan T M and Schalk G 2003 The Wadsworth Center brain–computer interface (BCI) research and development program *IEEE Trans. Neural Syst. Rehabil. Eng.* **11** 204–7

[19] Wolpaw J R, McFarland D J and Vaughan T M 2000 Brain–computer interface research at the Wadsworth Center *IEEE Trans. Rehabil. Eng.* **8** 222–6

[20] Pfurtscheller G *et al* 2000 Current trends in Graz brain–computer interface (BCI) research *IEEE Trans. Rehabil. Eng.* **8** 216–9

[21] Kostov A and Polak M 2000 Parallel man–machine training in development of EEG-based cursor control *IEEE Trans. Rehabil. Eng.* **8** 203–5

[22] Levine S P *et al* 2000 A direct brain interface based on event-related potentials *IEEE Trans. Rehabil. Eng.* **8** 180–5

[23] Pfurtscheller G, Graimann B, Huggins J E, Levine S P and Schuh L A 2003 Spatiotemporal patterns of beta desynchronization and gamma synchronization in corticographic data during self-paced movement *Clin. Neurophysiol.* **114** 226–36

[24] Levine S P *et al* 1999 Identification of electrocorticogram patterns as the basis for a direct brain interface *J. Clin. Neurophysiol.* **16** 439–47

[25] Huggins J E *et al* 1999 Detection of event-related potentials for development of a direct brain interface *J. Clin. Neurophysiol.* **16** 448–55

[26] Rohde M M *et al* 2002 Quality estimation of subdurally recorded, event-related potentials based on signal-to-noise ratio *IEEE Trans. Biomed. Eng.* **49** 31–40

[27] Pfurtscheller G and Cooper R 1975 Frequency dependence of the transmission of the EEG from cortex to scalp *Electroencephalogr. Clin. Neurophysiol.* **38** 93–6

[28] Marple S L 1987 *Digital Spectral Analysis with Applications* (Englewood Cliffs, NJ: Prentice-Hall)

[29] Wonnacott T H and Wonnacott R 1977 *Introductory Statistics* (New York: Wiley)

[30] Pfurtscheller G and Aranibar A 1977 Event-related cortical desynchronization detected by power measurements of scalp EEG *Electroencephalogr. Clin. Neurophysiol.* **42** 817–26

[31] Pfurtscheller G 1992 Event-related synchronization (ERS): and electrophysiological correlate of cortical areas at rest *Electroencephalogr. Clin. Neurophysiol.* **83** 62–9

[32] McFarland D J, Miner L A, Vaughan T M and Wolpaw J R 2000 Mu and beta rhythm topographies during motor imagery and actual movements *Brain Topogr.* **12** 177–86

[33] Neuper C, Muller G R, Kubler A, Birbaumer N and Pfurtscheller G 2003 Clinical application of an EEG-based brain–computer interface: a case study of a patient with severe motor impairment *Clin. Neurophysiol.* **114** 399–409

[34] Wolpaw J R, Flotzinger D, Pfurtscheller G and McFarland D J 1997 Timing of EEG-based cursor control *J. Clin. Neurophysiol.* **14** 529–38

[35] Penny W D, Roberts S J, Curran E A and Stokes M J 2000 EEG-based communication: a pattern recognition approach *IEEE Trans. Rehabil. Eng.* **8** 214–5

[36] Kubler A *et al* 1999 The thought translation device: a neurophysiological approach to communication in total motor paralysis *Exp. Brain Res.* **124** 223–32

[37] Wolpaw J R and McFarland D J 1994 Multichannel EEG-based brain–computer communication *Electroencephalogr. Clin. Neurophysiol.* **90** 444–9

[38] Wolpaw J R and McFarland D J 2003 Two-dimensional movement control by scalp-recorded sensorimotor rhythms in humans *Abstract Viewer/Itinerary Planner* (Washington, DC: Society for Neuroscience) program no 607.2.2003

[39] Fetz E E and Finocchio D V 1971 Operant conditioning of specific patterns of neural and muscular activity *Science* **174** 431–5

[40] Lopes da Silva F H and Pfurtscheller G (ed) 1999 Event-related desynchronization *Handbook of Electroencephalography and Clinical Neurophysiology* (Amsterdam: Elsevier)

[41] Pfurtscheller G 1977 Graphical display and statistical evaluation of event-related desynchronization (ERD) *Electroencephalogr. Clin. Neurophysiol.* **43** 757–60

[42] Crone N E *et al* 1998 Functional mapping of human sensorimotor cortex wirh electrocorticographic spectral analysis: I. Alpha and beta event-related desynchronization *Brain* **121** 2271–99

[43] Schalk G, McFarland D J, Hinterberger T, Birbaumer N and Wolpaw J R 2004 BCI2000: a general purpose brain–computer interface (BCI) system *IEEE Trans. Biomed. Eng.* at press

[44] Aoki F, Fetz E, Shupe L, Lettich E and Ojemann G A 1999 Increased gamma-range activity in human sensorimotor cortex during performance of visuomotor tasks *Clin. Neurophysiol.* **110** 524–37

[45] Ramoser H, Wolpaw J R and Pfurtscheller G 1997 EEG-based communication: evaluation of alternative signal prediction methods *Biomed. Tech.* **42** 226–33

[46] McFarland D J and Wolpaw J R 2003 EEG-based communication and control: speed-accuracy relationships *Appl. Psychophysiol. Biofeedback.* **28** 217–31

[47] Fox P T, Perlmutter J S and Raichle M E 1985 A stereotactic method of anatomical localization for positron emission tomography *J. Comput. Assist. Tomogr.* **9** 141–53

[48] Talairach J and Tournoux P 1988 *Co-Planar Sterotaxic Atlas of the Human Brain* (New York: Thieme Medical)

[49] Collins D L *et al* 1998 Design and construction of a realistic digital brain phantom *IEEE Trans. Med. Imaging* **17** 463–8